Proceedings of the 21st ICSMGE, Vienna, Austria, 14 – 19 June 2026. Pistrol, Adam & Schweiger (eds.)
Published by: ÖGG, Austrian Society for Geomechanics, Salzburg, Austria, ISBN 978-3-9503898-4-5
https://doi.org/10.53243/ICSMGE2026-1911

Numerical modelling 2D vs. 3D: practice-oriented strategies for efficient numerical modelling in geotechnical engineering

Nataly Filipouskaya
Ramboll Deutschland GmbH, Hamburg, Germany, nataly.filipouskaya@ramboll.com

Prof. Dr.-Ing. Tim Pucker
HafenCity University, Hamburg, Germany

Lukas Brodersen
Wasserstraßen-Neubauamt, Hannover, Germany

ABSTRACT: With the advancement of 3D building information modelling, there is increasing interest in complex cross-disciplinary 3D models, including numerical modelling. 3D Finite Element (FE) models are sometimes mistakenly considered "more accurate and better", making them a preferred choice. This preference is based on their ability to account for 3D effects such as geometry, loads, soil stratification, and the interaction of individual components or objects. However, attempting to create an all-encompassing 3D FE model can contradict the core principle of numerical modelling. Effective numerical models rely on using symmetries and reducing complexity to the necessary level. Additionally, the level of detailing in a 3D FE model is limited by the capabilities of the hardware and software, as well as the rules of numerical modelling. Consequently, when starting to simplify a 3D FE model, the desired level of detail and accuracy can quickly be lost. This study explores how to select an appropriate and efficient method for numerical modelling in geotechnical engineering. Practical examples are drawn from the large-scale project of the Lüneburg Lock (Schleuse Lüneburg) in northern Germany. The findings highlight what has proven to be effective and what has been less successful in practice.

KEYWORDS: Finite element modelling, Plaxis, Lüneburg Lock, Scharnebeck twin ship lift, deep excavations

1 INTRODUCTION

The Lüneburg Lock project (or Schleuse Lüneburg in German) is aptly called a project of the century. Located in northern Germany on the Elbe Lateral Canal, connecting the Port of Hamburg with inland ports, the new lock is planned to facilitate the increasing demand for the transportation of various cargo via the country's inland waterways. With 225-meter-long, 12.5-meter-wide basins and a 38-meter water level difference, the Lüneburg Lock will be one of the largest locks of its kind in Europe.

The new lock will initially support and eventually replace the existing Scharnebeck ship lift. The twin counterweight lift, constructed in 1974, was the largest ship lift in the world at that time. However, with the ever-growing amount of traffic and the increasing length of cargo vessels, the Scharnebeck ship lift can no longer provide sufficient capacity.

The construction of the new lock will take place at a short distance from the existing ship lift while the lift remains in operation. Consequently, a significant focus is placed on the prediction of possible ground movements during the excavation, construction, and operation of the new lock and the connecting harbors. As a result, it was decided at an early stage of the project to apply numerical Finite Element Modelling (FEM) with the software packages Plaxis 2D and 3D (Bentley Systems, 2024) to assess the interaction between several parts of the new project and the existing structures as well as the resulting deformations.

The objectives of this paper are to provide a comprehensive overview of the simulations performed for the Lüneburg Lock project, explain the application and challenges of large-scale 3D FE models, evaluate the benefits and limitations of simpler 2D models, and compare the project specific calculation results between 3D and 2D FE models. Insights and recommendations will be offered on selecting efficient numerical modelling techniques.

2 LÜNEBURG LOCK PROJECT ELEMENTS

The scope of the Lüneburg Lock project encompasses the following project element (Figure 1):

- Deep excavation for the new lock
- Extension of upper and lower harbors
- Dam for the extended upper harbor
- Canal bridge for the entrance of the lock
- Retaining walls for temporary roads

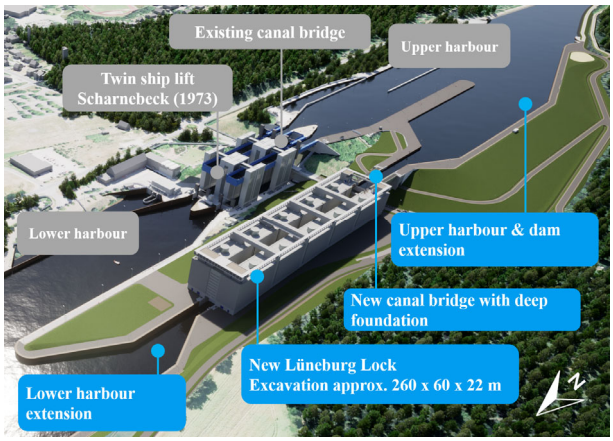

Figure 1. Overview of the project incl. existing and new structures

The excavation for the new lock is an approx. 30 m deep pit with diaphragm walls (D-walls), braced by concrete struts, underwater concrete floor (UWCF) and tension piles against uplift. Its proximity to the existing ship lift (the excavation is located about 60 m to the west of the existing structure) shifts the focus towards numerical calculations, aiming to assess the possible ground movements. The soil-structure interaction and the design of the excavation is also assessed with the numerical simulations, e.g. by calculating earth pressures, bedding stiffnesses, internal forces and deformations of the D-walls with the FEM.

The 25 m high upper dam will be constructed using the excavated soil material (approx. 755.000 m³). The dam is required for expansion of the upper harbor and construction of the entrance to the new lock.

The canal bridge is a structure with a span of about 48 m, that allows ships to enter the lock. On one side the support of the bridge is integrated into the lock wall. The other side is a bridge abutment with a piled foundation.

2.1 *Construction phases*

The construction phases of the new lock Lüneburg, that are considered in the FE analyses, include a total of 13 stages: 9 excavation stages and 4 lock construction stages.

BZ 0-1: Excavation of the working area at +12 mNHN
BZ 0-2: Installation of the D-walls
BZ A-1: First level excavation down to +9 mNHN
BZ A-1-1: Installation strutting system and tension piles
BZ A-2: Second level of excavation down to -2 mNHN
BZ B-1: Final excavation level -10.5 mNHN
BZ B-1-1: Construction dam
BZ B-2: Casting of the underwater concrete floor (UWCF)
EZ: Dewatering of the excavation pit
RB 0: 1st stage casting: foundation of the new lock
RB 2.1: 2nd stage casting: casting of the walls
RB 4.2: Removal of the struts
FSt: Completion of the lock

3 GROUND CONDITIONS

3.1 *3D geological model in Leapfrog*

The site investigation campaign comprised of 66 CPTs and 94 borehole explorations. The data was transferred into a 3D ground model, developed with the software package Leapfrog Works (Seequent, 2021). The 3D ground model replaces the conventional 2D sectional drawings. Furthermore, it allows for more precise 3-dimensional ground interpretation and a spatial definition of soil lenses.

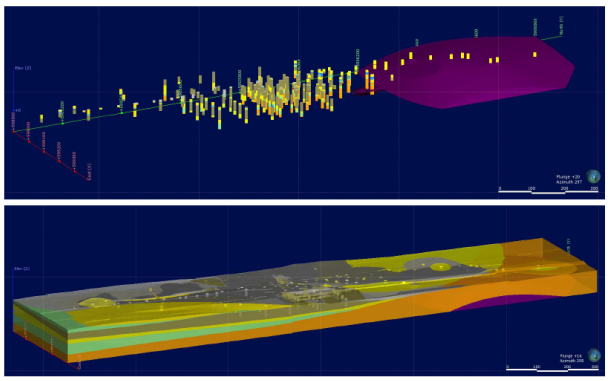

Figure 2. 3D ground model in Leapfrog

3.2 *Ground characteristics*

The ground is characterized predominantly by dense sands and gravels, basin silts and locally formed lenses of glacial till and tertiary clay. Except for the upper sands and man-made fills, the soil units are assumed to be overconsolidated, with overconsolidation ratios (OCR) reaching from 6 to 8. The general set of soil parameters based on geotechnical interpretative report (GIR) is shown in Table 1.

Table 1. General soil parameters

Soil unit	γ / γ' [kN/m³]	φ' [°]	c' [kPa]	E_s [MPa]	OCR [-]
Fill and upper sands, medium dense	18.5 / 10.5	35	0	50	1
Glacial sands, dense to very dense	19 / 11	37.5	0	80	8
Glacial sand & gravel, dense to very dense	19 / 11	37.5	0	80	7
Basin sand, very dense	19.5 / 10.5	39	0	140	5
Basin silt	20.5 / 10.5	35	10	35	6
Glacial till	22 / 12	35	5	30	7

3.3 *Groundwater*

There is a distinct groundwater flow from south to north, from the upper canal to the lower canal with a head difference of roughly 8 m. By constructing the new lock, the retaining walls of the excavation create a barrier for the groundwater flow leading to increase in groundwater level on the southern side of the excavation and a drop in groundwater level at the opposite side.

Furthermore, there is a confined aquifer in the underlying basin sands with the pressure head reaching nearly the ground surface level.

3.4 *Constitutive models for FEM*

The Hardening Soil – small strain (HSS) model (Brinkgreve, 2012) was used to simulate the ground behavior in the FE models.

In addition to the soil parameters provided with the GIR, laboratory tests (triaxial and oedometer) as well as crosshole seismic data were evaluated to calibrate the parameters required for the HSS constitutive model. It is important to emphasize that calibrating a constitutive model based on available laboratory and in-situ data is a critical step in numerical modelling, particularly when accurate predictions of deformations and settlements are required. The calibrated parameters for HSS soil model are included in Table 2.

Table 2. Calibrated soil parameters for HSS soil model

Soil unit	ψ [°]	$E_{50,ref}$ / $E_{OED,ref}$ / $E_{ur,ref}$ [MPa]	$G_{0,ref}$ [MPa]	$\gamma_{0,7}$ [-]	m [-]
Fill and upper sands, medium dense	5	33.6 / 33.6 / 100.8	7.5	1.4e-4	0.52
Glacial sands, dense to very dense	7.5	45.6 / 45.6 / 136.8	80.4	1.2e-4	0.46
Glacial sand & gravel, dense to very dense	7.5	45.6 / 45.6 / 136.8	87.1	1.2e-4	0.46
Basin sand, very dense	9	52.8 / 52.8 / 158.4	94.5	1.2e-4	0.42
Basin silt	7.4	15 / 8.25 / 65	93.1	2.1e-4	0.7
Glacial till	3.1	14.0 / 6.0 / 60.0	38.8	1.7e-4	0.7

The application of OCR values greater than 1 in the numerical models in Plaxis leads to several effects, some of which may be undesirable. In addition to the expected increase in soil stiffness, OCR also influences the coefficient of earth pressure at rest K_0.

Empirical approaches proposed for determining K_0^{OC}, such as those by Mayne & Kulhawy (1982), Mader (1989), and Pelz (2010), specify the coefficient of earth pressure at rest for

overconsolidated soils, K_0^{OC}, as a function of the OCR. In the impmented version of the HSS model in Plaxis, it is the Poisson's ratio ν_{ur} that significantly influences K_0^{OC} during unloading and reloading:

$$\frac{\sigma'^0_{xx}}{\sigma'^0_{yy}} = K_0^{NC} OCR - \frac{\nu_{ur}}{1-\nu_{ur}}(OCR-1) \quad (1)$$

As Figure 3 shows, the variation of Poisson's ratio directly impacts the stress state during both loading and reloading phases in overconsolidated soils. Consequently, the calibration of the Poisson's ratio ν_{ur} is essential to achieve a realistic simulation of soil behavior. The calibrated values from the project Lüneburg Lock are presented in Table 3.

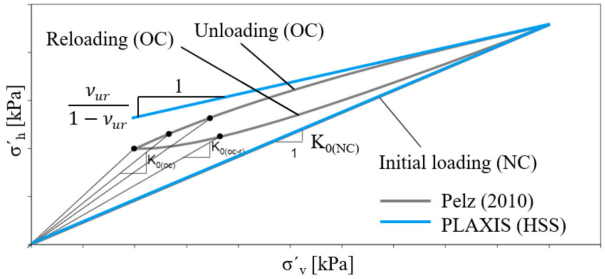

Figure 3. Stress relationship in initial loading, unloading and reloading incl. component of Poisson´s ratio in HSS model in Plaxis.

Table 3. Calibrated Poisson's ratio for HSS soil model

Soil unit	ν' [-]	OCR
Fill and upper sands, medium dense	0.2	1
Glacial sands, dense to very dense	0.24	8
Glacial sand & gravel, dense to very dense	0.23	7
Basin sand, very dense	0.21	5
Basin silt	0.22	6
Glacial till	0.23	7

4 NUMERICAL MODELS

4.1 *General*

The numerical modelling is performed with the software packages Plaxis 2D and 3D (Bentley Systems, 2024). The parameters for soil constitutive models, interfaces and structural elements are nearly identical, except for definition of the tension piles.

The wide spectrum of soil-structure interaction topics is assessed in detail using 2D modelling at selected cross sections. Different soil conditions are recreated using four cross sections of the 255-meter-long excavation and one longitudinal section. These 2D Plaxis models assess the following design aspects and topics:

- Horizontal bedding stiffness for the D-wall embedment.
- Earth pressure on the D-wall considering the construction phases, stepwise excavation of the pit, dewatering, system change due to hardening of the UWCF and concrete casting for the new lock structure.
- Deformation of the D-wall during each construction phase.
- Internal forces (shear and bending moments) of the D-walls.
- Bedding stiffness for the new lock.
- Settlements of the new lock during construction phases, during operation and maintenance load cases.

The calculated results are further used as input for structural design as well as planning and decision making of the construction phases.

Due to the proximity of several project elements, including the existing structures of the ship lift and the harbors, the interaction between these elements is crucial and highly focused upon. As a result, the project scope specifically included the requirement for a large-scale 3D numerical model that incorporates all relevant project elements and construction phases. The challenge of this type of numerical modelling, besides the obvious complexity and the number of structures to be included, is the sheer size of the model domain needed and the required computational power.

4.2 *Global 3D FE model of Lüneburg Lock*

The global 3D FE model for the Lüneburg Lock covers the area of 0.32 km² or 400x800 m. The boundaries of the modelling domain are set sufficiently far away from the zones of interest to eliminate boundary effects. The extent of the boundaries is determined by sensitivity analyses. The aim of the global 3D FE model is to register overall interactions between the structures on a higher-level as well as to address the effects on the existing ship lift at each construction phase.

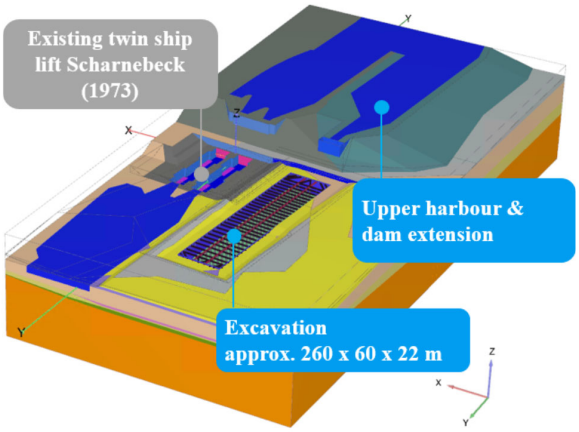

Figure 4. Global 3D FE model in Plaxis

4.3 *Soil layering in FE models*

The 3D ground model in Leapfrog forms the basis for soil layering. For 2D analyses, various sections are exported from the ground model.

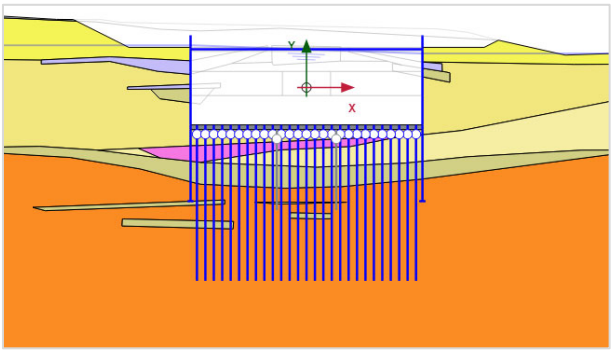

Figure 5. Excavation model in Plaxis 2D with the complex soil layering and lenses

A complex soil layering including lenses, as shown in Figure 5, could be implemented in Plaxis 2D without a major impact on the calculation time and the quality of the mesh. While the necessity of such a high level of precision in geotechnical and structural design may be debatable, it is nevertheless technically feasible and is handled effectively by the software.

The implementation of soil layering in Plaxis 3D is significantly more complex. The surfaces that can be exported from the Leapfrog ground model require further processing before they can be imported into Plaxis 3D.

Surfaces generated in Leapfrog typically contain a high density of nodes and complex curvatures, resulting in a level of detail that exceeds the requirements—and often the capabilities—of finite element (FE) analysis. The objective is to simplify the surface geometry and reduce node density in areas where high precision is unnecessary, while preserving critical edges and key nodal features essential for accurate modelling. However, the adjustment and manipulation of surface geometries in Plaxis are limited by the absence of adequate tools and functions necessary for efficient processing.

Currently, the most practical solution involves an intermediate step using Rhinoceros 8 (Robert McNeel & Associates, 2023) software package to process the surface by reducing the mesh and transforming it into a Non-uniform Rational Basis Spline (NURBS) surface. Alternatively, without additional software, a point cloud can be imported directly into Plaxis 3D, where it automatically creates a NURBS surface. Subsequently, the NURBS surface discretization can be adjusted within Plaxis 3D. However, this solution results in significant precision loss, potentially causing important edges of the surface to become smeared and lost.

In Plaxis, the inclusion of 14 digits after the decimal point for coordinate precision can result in virtually identical nodes being disconnected. This disconnection impedes intersections, leads to non-watertight geometries and issues with mesh generation. The high precision of coordinates is a likely reason why imported geometry from external CAD software often results in corrupted surface geometries, non-watertight volumes, and meshing issues. A practical solution is to use a parametric, coordinate-based geometry definition via the command line or Python interface.

In the global 3D FE model for Lüneburg Lock, the soil layering was adjusted so that the relevant areas of the model maintained a significant level of detail, while the areas outside of focus were simplified, as presented in Figure 6 to Figure 9. For the design of the excavation, the critical section was identified at the southern D-wall (Figure 6), due to its close proximity to the dam, the largest excavation level and the highest design groundwater pressure defined for this area.

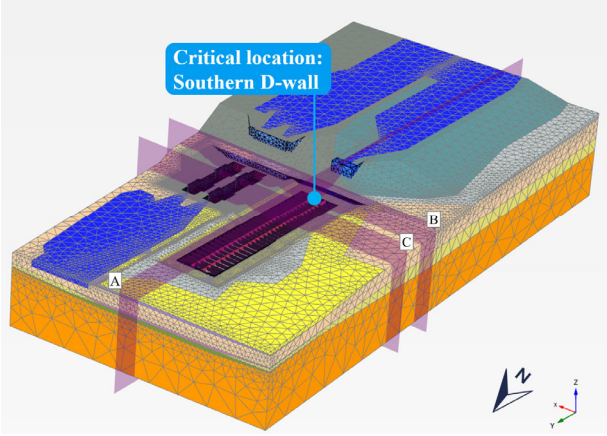

Figure 6. Global 3D FE model with sections A-A, B-B, C-C

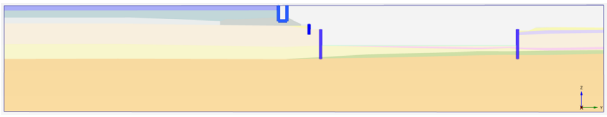

Figure 7. Longitudinal section A-A crossing the dam, the canal bridge and the excavation. Structural elements are blended out.

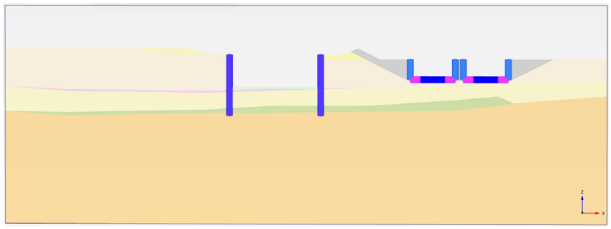

Figure 8. Section B-B crossing the excavation and existing ship lift. Structural elements are blended out.

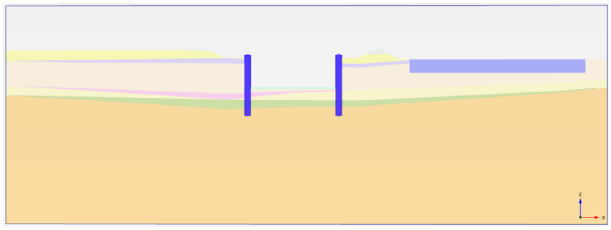

Figure 9. Section C-C crossing the excavation. Structural elements are blended out.

5 COMPARING AND COMBINING RESULTS OF 2D AND 3D FEM

5.1 *Soil-structure interaction of the excavation*

The structural design of the Lüneburg Lock excavation included soil-structure interaction effects by applying horizontal earth pressures from FE analysis into analytical design tools like GGU-Retain software. Initially, earth pressure distribution followed EAB (2021) recommendations was applied and adjusted with a phase-specific factor based on FE analysis results.

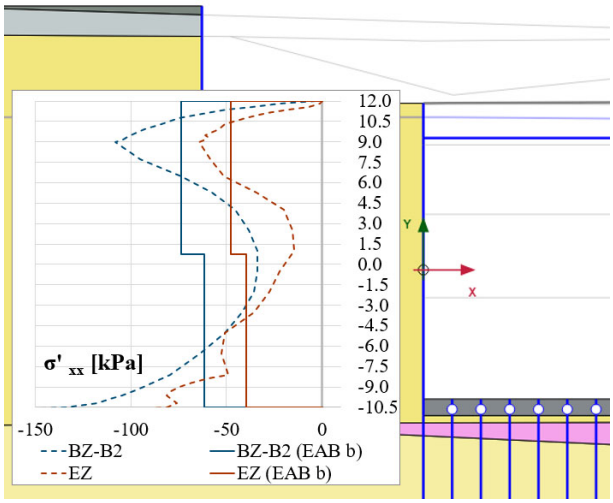

Figure 10. Effective earth pressure from Plaxis 2D model (southern D-wall) for the construction stages BZ-B-2 (full excavation) and EZ (dewatered pit). The solid lines represent the re-distributed earth pressure method according for EAB, type b.

Figure 10 shows an example of derivation of the effective earth pressure in the stages BZ-B-2 and EZ for the south wall of the excavation. In the stage BZ-B2 the full excavation depth is reached and UWCF is activated, while in EZ the pit is dewatered. As the hydrostatic water pressure on the outside of the excavation causes further horizontal displacement of the wall, the effective earth pressure on the active side reduces. In the current example, the reduction of the earth pressure of approx. 35% was taken into account, which allowed for an optimization of the structural D-wall design.

Furthermore, the 2D FE Plaxis models are used for the evaluation of the structural forces and deformations of the D-

walls. After the casting of the UWCF, the static system of the wall transitions from the soft bedding stiffness of the ground embedment to the stiff support of the UWCF. The resulting internal forces and bending moments are a combination of the two systems. Figure 11 shows the bending moments of the southern D-wall for construction phases BZ-B-2 and EZ, as well as the difference between the two. It illustrates the effects of the change in the static system with the buildup of the bending moment over the UWCF support point. The structural design tools often neglect the staged construction sequence, making them unable to account for these effects.

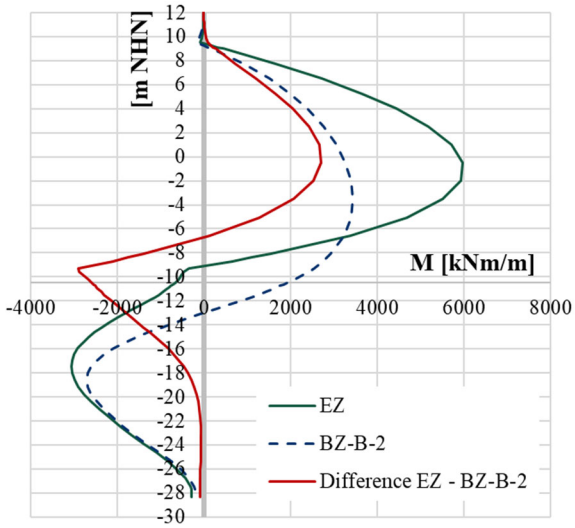

Figure 11. Bending moment of the southern D-wall

The bending moments of the D-walls in the 3D FE model of the excavation indicate the highest bending moments at the southern wall, confirming the section to be most critical for the design (Figure 12 and Figure 13). Table 4 summarizes the results relevant to the structural design of the excavation, comparing the 2D and 3D FE analyses.

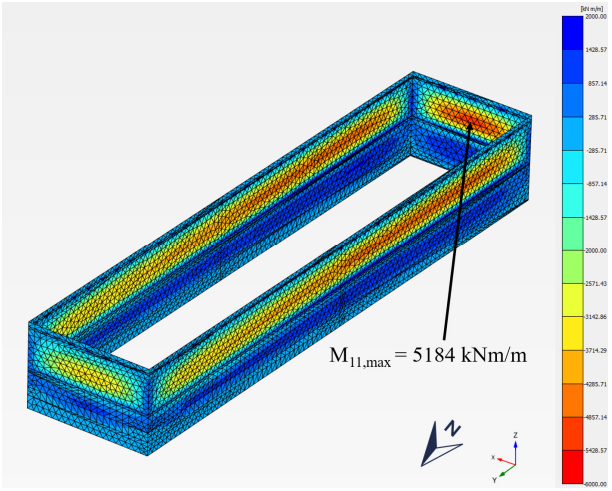

Figure 12. Bending moments of the D-walls for the stage EZ.

Figure 13. Horizontal section through the D-walls at z = -0.80 m for the maximum bending moments.

Table 4. Comparison of the results from 2D and 3D FEM for the structural excavation design

	2D FEM	3D FEM	Deviation [%]
Max. Bending moments of the D-walls [kNm/m]	5978	5184	13% ↓
Min. Bending moments of the D-walls [kNm/m]	-3057	-1373	55% ↓
Wall deformation [cm]	8.21	4.61	43% ↓
Max. strut force, longitudinal [MN]	9.60	9.55	0.5% ↓
Max. strut force, transverse [MN]	8.16	8.11	0.6% ↓
Max. strut force, corner [MN]	-	16.42	-

Overall, the 2D FE model yields more conservative results, particularly regarding the deformation of the southern D-wall (Figure 14). With an aspect ratio of 2.7 > 2 (length-to-width), the southern wall meets the definition of a one-way spanning slab. However, the bending behavior is likely influenced by transverse spanning and the 3D load distribution effects typical of a plate supported in two directions. Furthermore, in 3D the influence of the dam load is confined to the actual dam geometry, whereas in the 2D cross section the dam volume tends to be overestimated.

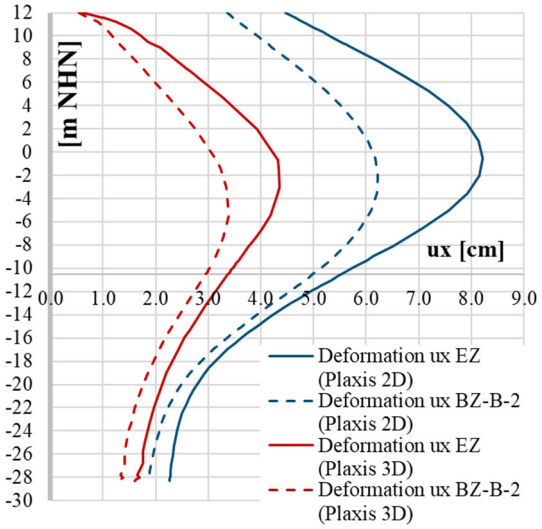

Figure 14. D-wall deformation, comparing 2D and 3D FEM results

The 3D FE model enables the evaluation of excavation corners, such as extracting corner bracing forces, as well as verifying critical section assumptions, while identifying inconsistencies and potential weak points. The 3D FE model enables the evaluation of excavation corners, such as extracting corner bracing forces, as well as verifying critical section assumptions, while identifying inconsistencies and potential weak points. While it allows for the assessment of 3D effects, the discretization of the 3D FE model is significantly coarser, potentially leading to less precise results. Consequently, 2D models are employed for detailed analyses, providing a more focused and accurate approach.

5.2 *Interaction between the dam and excavation*

The effects of the dam construction adjacent to the excavation pit, considering the construction sequence, were assessed using a global 3D FE model. In 2D FE models, the volume of the dam and its surcharge load are often overestimated, leading to a rather conservative wall design. Conversely, the 3D FE model

allows for a more precise representation of the dam geometry and facilitates a three-dimensional load distribution.

Overall, the dam contributes about 9% to the bending moment of the southern D-wall (Figure 15).

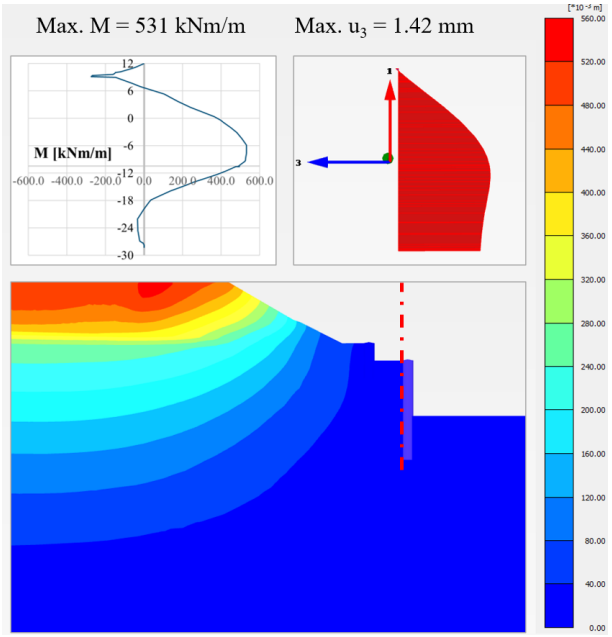

Figure 15. Interaction of the dam and the southern D-wall

5.3 *Effects on the existing ship lift*

The allowable deformations of the existing ship lift are limited and must be carefully evaluated during both the construction phases and final operation of the new Lock Lüneburg. In the 3D FE model, each construction phase is evaluated for overall displacement within the model domain, including the displacements of the existing ship lift structure. The location of the ship lift within the model domain is identified in Figure 16.

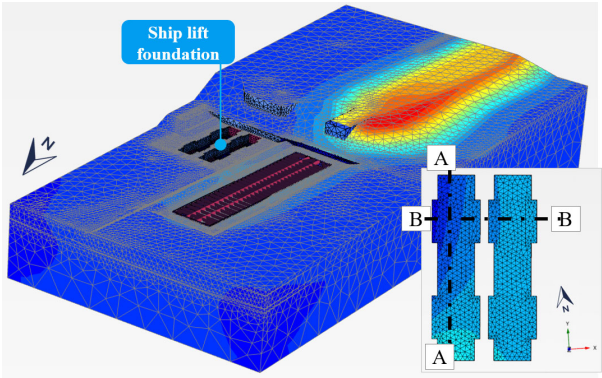

Figure 16. Location of the ship lift structure in the global 3D FE model. Location of the sections A-A and B-B through the ship lift foundation.

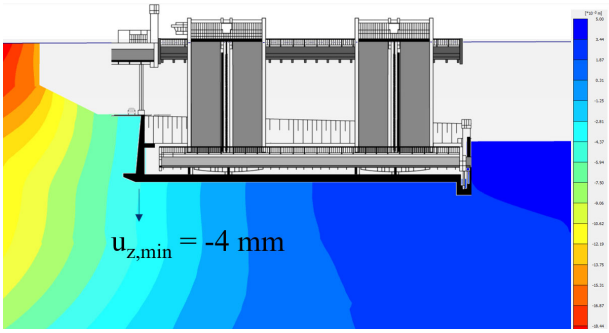

Figure 17. Section A-A through the ship lift foundation: settlement (-)/ heave (+) u_z [mm] during construction (EZ)

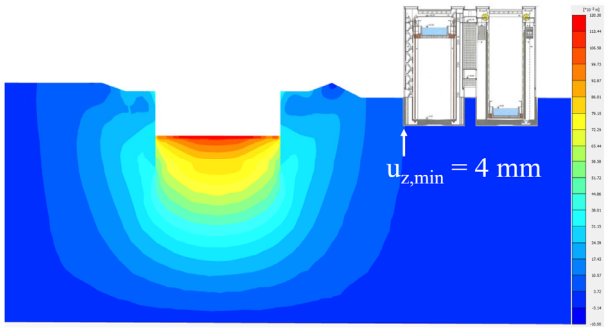

Figure 18. Section B-B through the ship lift foundation: settlement (-)/ heave (+) u_z [mm] during construction (EZ)

The evaluation of vertical displacements (Figure 17, Figure 18) during the final construction phase (EZ) indicates that one side of the ship lift undergoes settlements, primarily due to the added mass from the dam construction. Conversely, the opposite side of the ship lift tends to heave as a result of unloading during the excavation phase and dewatering of the excavation pit. The vertical displacement values remain within the magnitude of 4 mm, which is acceptable for the construction of this scale.

6 CONCLUSIONS

The Lüneburg Lock project highlighted the importance of selecting appropriate numerical modelling techniques. Both 3D and 2D finite element models were utilized, each offering unique advantages.

3D FE models provided insights into complex interactions and three-dimensional load distribution, despite their coarser discretization. In contrast, the 2D FE simulations allowed a finer mesh and the explicit representation of heterogeneous soil layers and lenses, which in turn facilitated targeted parametric studies and rapid iterative design cycles.

The complementary use of 3D and 2D models therefore provided a resilient design methodology that effectively met the project's geotechnical challenges. Future work should concentrate on refining key modelling assumptions and corroborating numerical predictions with field monitoring and other empirical data.

7 ACKNOWLEDGEMENTS

The author gratefully acknowledges the co-authors for their constructive feedback. Special thanks are extended to the Plaxis support team for their technical assistance throughout the modelling process.

8 REFERENCES

Bentley Systems. 2024. PLAXIS 2D Version 2024.2 Tutorial Manual.
Bentley Systems. 2024. PLAXIS 3D Version 2024.2 Tutorial Manual.
Brinkgreve, R.B.J., Engin, E., Swolfs, W.M. 2012. Plaxis 3D material models manual.
EAB, 2021. Deutsche Gesellschaft für Geotechnik e.V. Empfehlungen des Arbeitskreises Baugruben (EAB). 3rd Edition. Ernst & Sohn.
Mader, H. 1989. Untersuchungen über den Primärspannungszustand in bindigen überkonsolidierten Böden am Beispiel des Frankfurter Untergrundes. Mitteilungen des Institutes für Grundbau, Boden- und Felsmechanik TH Darmstadt, Heft 29.
Mayne, P.W., and Kulhawy, F.H. 1982. K0-OCR Relationships in soil. Journal of Geotechnical Engineering, Vol. 108, No. GT6, 851-872.
Pelz, G. 2010. Die Berücksichtigung einer Vorbelastung bei der Mobilisierung des passiven Erddruckes feinkörniger Böden. TU Munich.
Robert McNeel & Associates, 2023. Software Rhinoceros 3D V8.
Seequent, 2021. Software Leapfrog Works Version 21.2.